Gondwana Research 23 (2013) 130–140

Contents lists available at SciVerse ScienceDirect

Gondwana Research

journal homepage: www.elsevier.com/locate/gr

Highly heterogeneous lithospheric mantle beneath the Central Zone of the North China Craton evolved from Archean mantle through diverse melt refertilization

Yan-Jie Tang *, Hong-Fu Zhang, Ji-Feng Ying, Ben-Xun Su, Zhu-Yin Chu, Yan Xiao, Xin-Miao Zhao

State Key Laboratory of Lithospheric Evolution, Institute of Geology and Geophysics, Chinese Academy of Sciences, P.O. Box 9825, Beijing 100029, China

ARTICLE INFO

Article history:
Received 30 September 2011
Received in revised form 14 December 2011
Accepted 21 January 2012
Available online 31 January 2012

Keywords:
Archean
Lithospheric mantle
Peridotite xenolith
Geochemistry
North China Craton

ABSTRACT

High-Mg# peridotite xenoliths in the Cenozoic Hebi basalts from the North China Craton have refractory mineral compositions (Fo > 91.5) and highly heterogeneous Sr–Nd isotopic compositions ($^{87}Sr/^{86}Sr = 0.7031–0.7048$, $^{143}Nd/^{144}Nd = 0.5130–0.5118$) ranging from MORB-like to EM1-type mantle, which are similar to those of peridotites from Archean cratons. Thus, the high-Mg# peridotites may represent relics of the ancient lithospheric mantle. Published Re–Os isotopic data for Cenozoic basalt-borne xenoliths show T_{RD} ages of 3.0–1.5 Ga for the peridotites from Hebi (the center of the craton), 2.2–0 Ga for those from Hannuoba and Jining (north margin of the craton), and 2.6–0 Ga for those from Fanshi and Yangyuan (midway between the center and north margin of the craton). In situ Re–Os data of sulfides in Hannuoba peridotites suggest that whole-rock Re–Os model ages represent mixtures of multiple generations of sulfides with varying Os isotopic compositions. These observations indicate that initial lithospheric mantle beneath the Central Zone of the North China Craton formed during the Archean and was refertilized by multiple melt additions after its formation. The refertilization became more intensive from the interior to the margin of the craton, leading to the high heterogeneity of the lithospheric mantle: more ancient and refractory peridotites with highly variable Sr–Nd isotopic compositions in the interior, and more young and fertile peridotites with depleted Sr–Nd isotopic composition in the margin. Our data, coupled with published petrological and geochemical data of peridotites from the Central Zone of the North China Craton, suggest that the lithospheric mantle beneath this region is highly heterogeneous, likely produced by refertilization of Archean mantle via multiple additions of melts/fluids, which were closely related to the Paleoproterozoic collision between the Eastern and the Western Blocks and subsequent circum-craton subduction events.

1. Introduction

Characterization of subcontinental lithospheric mantle has made contributions to our understanding of the formation and secular evolution of continents. Mantle xenoliths entrained in mantle-derived magmas are direct samples of lithospheric mantle and record wealth of information about the formation and evolution of the lithospheric mantle. Many investigations based on mantle xenoliths have shown that the North China Craton (NCC) has been severely destroyed during the Phanerozoic (e.g., Fan and Menzies, 1992; Griffin et al., 1992; Menzies et al., 1993; Griffin et al., 1998; Menzies and Xu, 1998; Fan et al., 2000; Xu, 2001; Wu et al., 2006; Zhang et al., 2007; Zheng et al., 2007; Xu et al., 2008a; Zhang et al., 2009; Xu et al., 2010). Diamond inclusions, mantle xenoliths and minerals xenocrysts in the Ordovician kimberlites indicate that the lithospheric mantle beneath the NCC was thick (about 200 km), cool (geotherms 36–40 mW/m^2), and typically Archean in compositions prior to the Paleozoic. However, the Tertiary basalt-borne xenoliths reveal the presence of thin (<80 km), hot (50–105 mW/m^2) and fertile lithosphere in the Cenozoic (Fan and Menzies, 1992; Menzies et al., 1993; Griffin et al., 1998; Menzies and Xu, 1998; Xu et al., 1998; Zheng et al., 1998; Fan et al., 2000; Xu, 2001; Gao et al., 2002; Zhang et al., 2009). This suggests the great changes in compositions and character of the lithospheric mantle during the Phanerozoic. Coupled with the changes is the widespread Mesozoic–Cenozoic magmatism (Zhou and Armstrong, 1982; Zhang et al., 2002; Yang et al., 2003; Zhang et al., 2003, 2004). Geochronological and geochemical studies of the igneous rocks and their mantle xenoliths have provided valuable information on the timing and mechanism of destruction of the NCC (e.g., O'Reilly et al., 2001; Xu, 2001; Gao et al., 2002; Zhang et al., 2002; Rudnick et al., 2004; Xu et al., 2004; Wu et al., 2006; Zheng et al., 2006; Menzies et al., 2007; Zhang et al., 2010a). However, the mechanism and process of the destruction are still subjects of considerable debate.

It should be noted that the NCC is divided into the Eastern and Western Blocks, separated by a Central Zone, and most of the above studies were based on the Eastern Block of the NCC (Fig. 1). Compared to the tectonothermal reactivation of the eastern NCC since

* Corresponding author. P.O. Box 9825, Beijing 100029, China. Tel.: +86 10 82998536; fax: +86 10 62010846.
E-mail address: tangyanjie@mail.igcas.ac.cn (Y.-J. Tang).

1342-937X/$ – see front matter
doi:10.1016/j.gr.2012.01.006

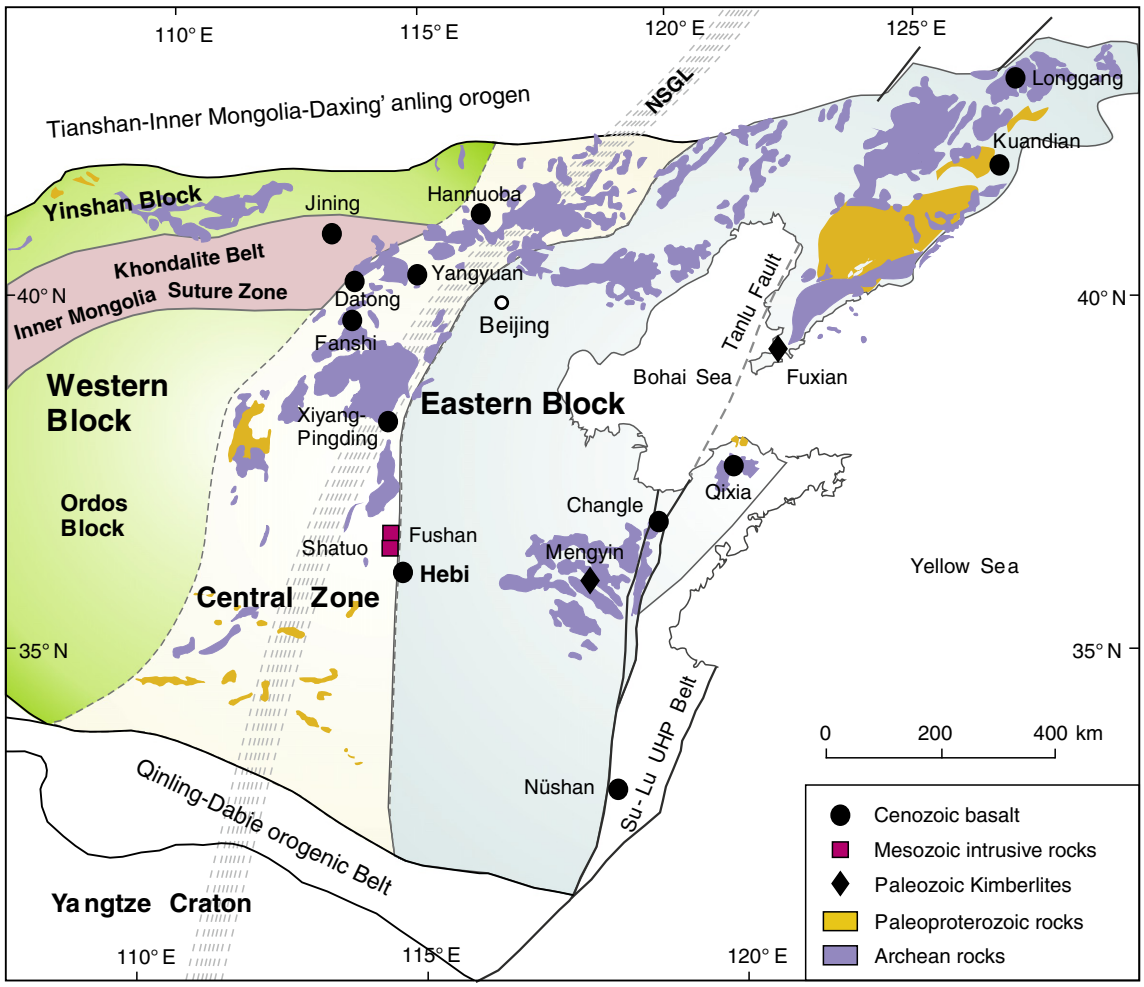

Fig. 1. Geologic and tectonic map of the North China Craton, revised after Zhao et al. (2000, 2008) and Santosh (2010), showing the distributions of the main tectonic subdivisions, rocks of different ages and mantle xenolith localities mentioned in the text. The NSGL represents the North–South Gravity Lineament (Ma, 1989).

the Mesozoic, the Western Block remains relatively stable since the Precambrian with only few magmatic activities. Thus, the Central Zone is the transitional zone of Phanerozoic magmatism, as well as crustal elevation, morphology, lithospheric thickness and gravity anomalies from the Eastern to the Western Block (Ma, 1989; Griffin et al., 1998; Menzies and Xu, 1998). Therefore, understanding the nature and evolution of the mantle lithosphere beneath the Central Zone is crucial to unravel mechanism and processes of destruction of the NCC. However, these aspects of the Central Zone are not well-constrained.

In this paper, we report the petrological and Sr–Nd isotopic compositions of peridotite xenoliths from Hebi County, Henan Province, which tectonically located in the east edge of the Central Zone (Fig. 1). Our main aim is to further constrain the nature and origin of the lithospheric mantle beneath the Central Zone by reviewing the data available for mantle xenoliths from the Central Zone of the NCC. Our study will provide an insight into the destruction of the NCC.

2. Geologic setting

The NCC is one of the Archean continental nuclei in the world and comprises three subdivisions (Fig. 1), i.e. the Eastern Block, the Central Zone and the Western Block (Zhao et al., 2000; Santosh, 2010; Kusky, 2011). The Western Block is composed of the Yinshan Block and the Ordos Block which were joined by the east–west trending Inner Mongolia Suture Zone at ~1.95 Ga (Santosh, 2010; Zhao et al., 2010a). This suture zone is also termed Khondalite Belt (Zhao et al., 2010a), with dominant lithology of graphite–garnet–sillimantie gneiss, garnet quartzite, felsic paragneiss, calc-silicate rock and marble. The basement of the Western Block mainly consists of granulite-facies tonalitic, trondhjemitic and granodioritic (TTG) gneisses and charnockites, which are unconformably overlain by Archean to Paleoproterozoic metasedimentary belts (Zhao et al., 2000). Paleoproterozoic ultrahigh temperature metamorphism has been observed in the Western Block (Santosh et al., 2007a, 2007b, 2009, 2011). The basement of the Eastern Block primarily consists of Archean TTG gneisses, granitoids, granitic gneisses and supracrustal rocks (Zhao et al., 2000).

The Central Zone is also called Trans-North China Orogen, roughly north–south trending across the NCC (Fig. 1). It consists of 2.5–2.7 Ga TTG gneisses, greenschist facies mafic rocks, amphibolites, high-pressure granulites and retrograded eclogites (Zhao et al., 2000; Zhang et al., 2006; Zhai and Santosh, 2011). This orogen was formed by the collision between the Eastern and the Western Blocks at about 1.85 Ga (Zhao et al., 2000, 2010a; Santosh, 2010), marking the formation of the NCC although the subduction polarity and the amalgamation timing of the various blocks remain debated (Kröner et al., 2005; Santosh, 2010; Zhao et al., 2010b; Kusky, 2011).

The Western Block remains relatively stable since the Precambrian and the lithosphere of this block is about 200 km thick. In contrast, the Eastern Block has experienced widespread tectono-thermal reactivation since the Late Mesozoic, as manifested by the emplacement of voluminous Late Mesozoic granites, mafic intrusions and volcanic rocks (Zhang et al., 2002, 2003; Yang et al., 2003; Zhang et al.,

2004) and extensive Cenozoic basalts (Zhou and Armstrong, 1982; Fan et al., 2000; Tang et al., 2006; Zhang et al., 2011). Ordovician diamondiferous kimberlites occur mainly in the Mengyin County, Shandong Province, and the Fuxian County, Liaoning Province in the Eastern Block (Fig. 1) (Dobbs et al., 1994). The lithosphere in these localities was cool and thick at the time of emplacement (Menzies et al., 1993; Griffin et al., 1998), with highly refractory compositions in mantle peridotites, indicating the existence of an Archean lithospheric keel beneath the Eastern Block at least until the kimberlite emplacement (Gao et al., 2002; Zheng et al., 2006; Zhang et al., 2008, 2009). In contrast, the Cenozoic basalts sampled a shallower and hotter lithosphere, with predominantly fertile compositions as manifested by the mantle peridotites (Fan et al., 2000; Zheng et al., 2001; Rudnick et al., 2004; Zhang et al., 2009), consistent with the geophysical observation of a thin lithosphere (80–60 km) in the Eastern Block (Yuan, 1996; Griffin et al., 1998; Chen et al., 2006). These observations suggest that the destruction of the NCC mainly occurred in the Eastern Block during the Phanerozoic.

The NEE-trending North–south Gravity Lineament (NSGL, Fig. 1) runs over 3500 km from south China to northeast China. It is a zone about 100 km wide, in which the Bouguer anomaly decreases rapidly from −100 mGal in the west to −40 mGal in the east (Ma, 1989). This gravity gradient roughly overlaps the Central Zone. To the east of the gravity lineament, the Eastern Block is characterized by a thin crust and lithosphere, high heat flow and weak negative to positive regional Bouguer anomalies; to the west of the gravity lineament, the Ordos nucleus has a thick crust and lithosphere, low heat flow and strong negative Bouguer anomalies (Ma, 1989; Yuan, 1996). The Hebi area of Henan province lies east of the gravity lineament and tectonically in the east edge of the Central Zone. Both Neogene basalts and Cretaceous–Eogene barren kimberlites occur in the Hebi. Olivine nephelinites are in 10 km south of Hebi city and have eruption ages of 4.0–4.3 Ma. The nephelinites contain abundant mantle xenoliths and megacrysts (up to 5 cm across) of garnet and pyroxene (Zheng et al., 2001). The kimberlites occur 6 km west of Hebi city and contain rare altered dunite and lherzolite xenoliths (Griffin et al., 1998).

3. Sample description and previous studies

Peridotite xenoliths in the Hebi Neogene olivine nephelinites are very fresh and belong to the Cr-diopside suite (Wilshire and Shervais, 1975). They range from 1 to 8 cm in diameter, with majority about 2 to 6 cm. The petrology, major- and trace-element, Re–Os, Li and Fe isotopic compositions of peridotite xenoliths from the Hebi have been studied previously (Zheng et al., 2001, 2007; Xu et al., 2008b; Zhao et al., 2010c; Liu et al., 2011; Tang et al., 2011). The Hebi peridotite xenoliths are dominant harzburgites with minor lherzolites. They can be divided into two groups based on the forsterite proportion in olivine (Fo): a low-Mg# group (Fo<91) and a high-Mg# group (Fo≥91). The low-Mg# peridotites are fertile (rich in basaltic components, such as Al_2O_3, Na_2O and CaO) in mineral compositions, typical of Phanerozoic mantle. The high-Mg# peridotites consist of highly refractory harzburgite (Al_2O_3 content<1.5%) and cpx-poor (cpx vol%<5%) lherzolites with coarse-grained and porphyroclastic structures, compositionally similar to xenoliths in kimberlites from Archean cratons. Thus the high-Mg# xenoliths have been interpreted as relics of the Archean cratonic mantle beneath the NCC (Zheng et al., 2001), and Re–Os isotopic data of the peridotites and their sulfides give Archean melt-extraction ages of 2.5–3.0 Ga (Zheng et al., 2007; Xu et al., 2008a). Li and Fe isotopic compositions of the Hebi peridotites suggest that the ancient lithospheric mantle beneath the Hebi experienced multistage metasomatism (Zhao et al., 2010c; Tang et al., 2011).

In this study, ten spinel-facies harzburgite xenoliths were selected for mineral chemical and Sr–Nd isotopic analyses. These samples are very fresh and 4–6 cm in diameter, with high modal opx (17–32%) and minor cpx contents (<4%; Table 1). Cpx is absent in some xenoliths. Most of the samples have coarse-grained structures and the olivine and opx grains are generally 3–6 mm in diameter, with maximum up to 10 mm. Porphyroclastic structures are also observed in these samples, with coarse olivine porphyroclasts in a matrix of fine-grained recrystallized/secondary minerals. Siliceous, aluminum- and alkali-rich glasses with fine-grained cpx phenocrysts are common in patches and small veins. Phlogopites are not observed in these samples.

4. Analytical methods

The xenoliths were sawn from their lava hosts and the cut surfaces were abraded with quartz to remove any possible contamination from the saw blade. The samples were crushed and sieved for mineral separation. Opx and cpx separates were handpicked under a binocular microscope to a purity of >99%.

Mineral modal contents have been determined by point-counting more than 1000 points in each thin section (Table 1). Major element compositions of minerals in the peridotite xenoliths were measured at the Institute of Geology and Geophysics, Chinese Academy of Sciences using a JEOL JXA8100 electron probe microanalyzer (EPMA). The operating conditions were as follows: accelerating voltage of 15 kV, 10 nA beam current, 5 μm beam spot and 10–30 s counting time. Natural minerals and synthetic oxides were used for standard calibration, and a program based on the ZAF procedure was used for data correction. The precisions of all analyzed elements are better than 1.5% based on multiple analyses of different grains within a sample.

Sr and Nd isotope compositions of cpx and opx separates from the xenoliths were determined at the Institute of Geology and Geophysics. The mineral separates were washed with 6 M HCl for 12 h and then ground to 200–400 mesh using an agate mortar before isotopic analysis. Analytical details for sample digestion, column separation and mass spectrometric measurement procedures are described in Chu et al. (2009a, 2009b). About 30–100 mg of cpx and 300–400 mg of opx powder was weighed into Teflon vials, and appropriate amounts of mixed ^{87}Rb–^{84}Sr and ^{149}Sm–^{150}Nd spikes were added. The samples were dissolved using a mixed acid of HF and $HClO_4$ on a hotplate at 120 °C for more than 1 week. After the samples were completely dissolved, the solutions were dried on hotplate at 130–180 °C to remove the HF and $HClO_4$. The sample residues were redissolved in 4 ml of 6 M HCl, and then dried again. Finally, the samples were dissolved in 2 ml of the 3% H_3BO_3 in 2.5 M HCl. The solutions were loaded onto pre-conditioned AG 50 W×12 columns for separation. Rb and Sr were stripped with 5 M HCl, and Nd and Sm were stripped with 0.14 M and 0.4 M HCl, respectively. The Rb, Sr, Nd and Sm were completely separated in our experiments.

The Rb–Sr and Sm–Nd isotopic analyses were performed on an IsoProbe-T thermal ionization mass spectrometer (GV instruments, England). Measured $^{87}Sr/^{86}Sr$ and $^{143}Nd/^{144}Nd$ ratios were corrected

Table 1
Mineral modes (vol.%) of the Hebi peridotites.

Sample	Olivine	Opx	Cpx	Spinel
05HB68	69	27	3	1
05HB70	79	18	1	2
05HB72	81	16	1	2
HB1120	77	22	0	1
HB1121	77	21	2	0
HB1122	73	24	1	2
HB1125	67	30	1	2
HB1126	71	27	1	1
05HB09	75	23	2	0
HB1128	70	29	0	1

for mass-fractionation using $^{86}Sr/^{88}Sr = 0.1194$ and $^{146}Nd/^{144}Nd = 0.7219$, respectively. During the period of data collection, the measured values for the NBS-987 Sr standard and the JNdi-1 Nd standard were $^{86}Sr/^{88}Sr = 0.710245 \pm 16$ (2 s, n = 8) and $^{143}Nd/^{144}Nd = 0.512117 \pm 10$ (2 s, n = 8), respectively. The USGS reference material BCR-2 was measured to monitor the accuracy of the analytical procedures. Our results are: 46.55 ppm Rb, 339.3 ppm Sr, $^{87}Sr/^{86}Sr = 0.704986 \pm 13$ (2 s), 6.543 ppm Sm, 28.60 ppm Nd, and $^{143}Nd/^{144}Nd = 0.512641 \pm 16$ (2 s). These values are comparable with the reported reference values: 45.5–48.5 ppm Rb, 312–355 ppm Sr, $^{87}Sr/^{86}Sr = 0.704958$–$0.705027$, 6.41–6.63 ppm Sm, 26.7–29.9 ppm Nd, and $^{143}Nd/^{144}Nd = 0.512633$–$0.512644$ (GeoREM, http://georem.mpch-mainz.gwdg.de/). The procedural blanks were 10, 49, 10 and 19 pg for Rb, Sr, Sm and Nd, respectively, which were less than 0.1% of the amount of samples loaded.

5. Results

5.1. Major elements

Olivine, opx, cpx and spinel in these peridotites xenoliths are homogeneous (2 s < 0.2) in major elemental compositions based on the determination of individual phases between core and rim. The average composition of 4–5 point analyses is presented in Table 2. Olivines in the xenoliths have high Fo (91.5–92.7) and low MnO (average 0.1%) and NiO (average 0.4%) contents. Opx minerals have high Mg# ranging from 91.9 to 92.7, low Al_2O_3 (2.0–3.4%) and CaO (0.3–1.1%) contents. Cpx minerals have Mg# varying from 92.1 to 93.2, Al_2O_3 of 3.0–4.6% and Cr_2O_3 of 1.1–2.2% (Table 2). Mineral modal contents (Fig. 2) and chemical compositions (Figs. 3–5) are similar to those of published high-Mg# peridotites from the Hebi (Zheng et al., 2001; Tang et al., 2011), harzburgite xenoliths entrained in the Cenozoic Fanshi (Tang et al., 2008, 2011) and Yangyuan basalts (Xu et al., 2008b) and Mesozoic Fushan diorites (Xu et al., 2010) in the Central Zone of the NCC (Fig. 1), which were interpreted as the residues of ancient lithospheric mantle.

5.2. Sr–Nd isotopic composition

Sr and Nd isotopic compositions of cpx and opx in the Hebi peridotites are given in Table 3 and illustrated in Fig. 6. They show a large variation ranging from MORB-like to high $^{87}Sr/^{86}Sr$ (up to 0.7044) and very low $^{143}Nd/^{144}Nd$ (down to 0.5118). Two samples display extremely low $^{143}Nd/^{144}Nd$ ratios relative to its Sr isotope ratios, having the signature of EM1-type mantle (Fig. 6). One sample falls within the field for the Mesozoic lithospheric mantle constrained by peridotite xenoliths (Xu et al., 2010) and mafic rocks (Zhang et al., 2004; Wang et al., 2006) from the Central Zone of the NCC (Fig. 6). In contrast, the cpx separates have higher Sr (most > 100 ppm) and Nd (most > 2 ppm) contents and relatively lower $^{87}Sr/^{86}Sr$ ratios (0.70309–0.70415) than the opx (Sr < 10 ppm, Nd < 0.3 ppm, $^{87}Sr/^{86}Sr = 0.70353$–$0.70483$). The opx are generally higher in Rb contents and Rb/Sr ratios than the coexisting cpx.

6. Discussion

6.1. Major element geochemistry and origin

Typical Archean cratonic mantle is generally composed of highly refractory (Fo > 92.5) harzburgites and cpx-poor lherzolites (Boyd, 1989), which are highly depleted in basaltic components due to high-degree melt extraction. In contrast, most Proterozoic and Phanerozoic lithospheric mantle worldwide are moderately depleted compared with primitive mantle (O'Reilly et al., 2001; Beyer et al., 2006). The Hebi peridotites studied here have high Fo (91.5–92.7) and thus are affiliated to the high-Mg# group (Fo > 91; Zheng et al., 2001). Their mineral modes are similar to those from the Archean Kaapvaal craton, South Africa (Fig. 2) and are plotted in the fields for the peridotite xenoliths from the Archean Siberian and Kaapvaal cratons (Fig. 3) (Griffin et al., 2003) and from the Paleozoic diamondiferous kimberlites in the NCC due to their refractory mineral compositions: high Fo and low MnO in olivine (Fig. 4), high Mg# and low Al_2O_3 in opx and cpx (Fig. 5). These characteristics are similar to those published for the Hebi high-Mg# peridotites, Fushan and Fanshi harzburgites, some Yangyuan peridotites and olivine xenocrysts from the Mesozoic and Cenozoic basaltic rocks in the Central Zone, which were considered as residues of the Archean lithospheric mantle (Zheng et al., 2001; Tang et al., 2004; Zheng et al., 2006; Tang et al., 2008; Xu et al., 2008b; Xu et al., 2010; Ying et al., 2010; Liu et al., 2011; Tang et al., 2011).

Therefore, the Hebi harzburgites represent residues of Archean lithospheric mantle beneath this region. Most of them have Fo lower than that of typical Archean cratonic mantle (Fo > 92.5; Boyd, 1989), indicating that the harzburgites were likely modified by melt–rock reaction, similar to those from the Archean cratons of Kaapvaal and Siberia, rather than the products of simple melt extraction (Kelemen et al., 1998; Zhang, 2009).

6.2. Sr–Nd isotopic compositions and mantle processes

The most striking character of Sr–Nd isotopic compositions of cpx in the Hebi harzburgites is the extreme heterogeneity. They display a large variation ranging from depleted-mantle to EM1-endmember compositions, similar to those of peridotites from ancient cratonic lithospheric mantle worldwide (Fig. 6). Since the changes in Rb/Sr and Sm/Nd ratios caused by mantle metasomatism will, with time, produce extreme isotopic heterogeneity, the cpx likely evolved from the mixing of a MORB-like lithospheric composition with several enriched components related to melt/fluid influx (Frey and Green, 1974). Melt/fluid derived from recycled or subducted materials may have considerable ranges in Sr/Nd ratios and isotopic compositions. This is evidenced by the large variations of isotopic compositions in the Late Mesozoic lavas of andesites, dacites and adakites (Zhang et al., 2003; Gao et al., 2004) and Hannuoba pyroxenite xenoliths (Xu, 2002) that involved recycled crustal components. As a result, the influx of recycled materials may account for the spread of the data (Fig. 6).

Two samples show an EM1-like isotopic signature of the Mesozoic lithospheric mantle beneath the same region (Fig. 6) that was considered to have been previously modified by silica-rich melts released from subducted materials (Wang et al., 2006; Tang et al., 2008). The subduction may be related to the Paleoproterozoic collision between the Eastern and the Western Blocks (Zhao et al., 2000; Santosh et al., 2010) because there is no evidence showing any collision in the interior of the NCC during the Phanerozoic. The EM1-type mantle beneath the Central Zone is also evidenced by the isotopic compositions of peridotite xenoliths from the Cenozoic Fanshi and Yangyuan basalts (Ma and Xu, 2006; Tang et al., 2007, 2008; Xu et al., 2008b), indicating a secular evolution of the subcontinental lithospheric mantle. This conclusion is also supported by the modeling calculations of the evolution of $^{143}Nd/^{144}Nd$ with time in the xenoliths assumed to have been modified by recycled crustal materials at 1.8 Ga (Fig. 7). Therefore, the enriched isotopic compositions in the Hebi harzburgites may reflect ancient enrichment processes of the Archean lithospheric mantle.

Some of the Hebi harzburgites have MORB-like Sr–Nd isotopic compositions of cpx (Fig. 6), indicating that these peridotites were modified by recent asthenospheric melt–peridotite reaction (Zhang, 2009), which is consistent with their relatively low Fo values (Fig. 8) and high concentrations of heavy rear earth elements as observed in the Fanshi peridotites (Tang et al., 2008). As stated above, the harzburgites are considered to be the relics of Archean

Table 2
Major elemental compositions (wt.%) of minerals in Hebi mantle xenoliths.

Sample	Mineral	SiO_2	MgO	FeO	CaO	Al_2O_3	Cr_2O_3	Na_2O	NiO	MnO	TiO_2	Total	Mg#
05HB68	Ol	41.42	49.70	7.97	0.07	0.06	0.03	0.01	0.35	0.12	0.02	99.8	91.8
05HB70	Ol	41.61	49.91	7.65	0.07	0.00	0.01	0.00	0.40	0.10	0.00	99.8	92.1
05HB72	Ol	41.62	50.11	8.14	0.10	0.00	0.07	0.00	0.37	0.12	0.00	100.5	91.7
HB1120	Ol	41.44	49.73	7.71	0.11	0.04	0.01	0.01	0.44	0.11	0.02	99.6	92.1
HB1121	Ol	41.38	50.36	8.05	0.11	0.03	0.02	0.02	0.40	0.11	0.00	100.5	91.8
HB1122	Ol	41.70	49.69	7.82	0.09	0.01	0.03	0.01	0.38	0.09	0.01	99.8	92.0
HB1125	Ol	41.16	49.27	8.07	0.11	0.00	0.00	0.03	0.31	0.12	0.01	99.1	91.7
HB1126	Ol	42.02	49.97	8.36	0.06	0.00	0.01	0.00	0.43	0.11	0.00	101.0	91.5
05HB09	Ol	41.56	50.29	7.92	0.08	0.03	0.00	0.00	0.40	0.12	0.00	100.4	92.0
HB1128	Ol	42.08	50.99	7.27	0.00	0.03	0.00	0.00	0.46	0.07	0.00	100.9	92.7
05HB68	Opx	56.28	32.88	4.96	1.07	3.17	0.82	0.02	0.13	0.15	0.00	99.5	92.3
05HB70	Opx	56.15	32.68	5.04	1.02	3.00	0.77	0.03	0.14	0.14	0.00	99.0	92.1
05HB72	Opx	55.89	32.99	4.81	0.96	3.44	0.91	0.13	0.13	0.13	0.02	99.4	92.5
HB1120	Opx	56.54	33.08	5.22	1.07	3.03	0.83	0.04	0.14	0.07	0.03	100.0	91.9
HB1121	Opx	56.06	33.04	4.84	0.97	3.16	0.84	0.05	0.10	0.13	0.01	99.2	92.5
HB1122	Opx	56.36	33.23	5.00	0.99	2.73	0.75	0.11	0.04	0.13	0.00	99.4	92.3
HB1125	Opx	56.49	33.49	4.78	0.84	2.74	0.83	0.07	0.11	0.08	0.00	99.4	92.7
HB1126	Opx	57.15	33.33	5.17	0.56	2.57	0.61	0.12	0.10	0.11	0.00	99.7	92.1
05HB09	Opx	56.24	33.49	5.03	0.99	2.78	0.84	0.02	0.12	0.11	0.01	99.6	92.3
HB1128	Opx	57.49	34.78	4.93	0.29	1.95	0.28	0.05	0.11	0.12	0.01	100.0	92.7
05HB68	Cpx	52.58	17.17	2.43	21.27	3.23	1.07	0.42	0.05	0.06	0.05	98.3	92.7
05HB70	Cpx	53.13	16.95	2.26	21.20	3.06	1.17	0.39	0.03	0.13	0.02	98.3	93.1
05HB72	Cpx	52.82	15.79	2.36	19.19	4.55	1.66	1.66	0.04	0.09	0.34	98.5	92.3
HB1120	Cpx	52.80	17.02	2.41	20.96	3.09	1.36	0.49	0.08	0.08	0.09	98.4	92.7
HB1121	Cpx	53.05	16.81	2.21	21.03	3.01	1.25	0.54	0.07	0.08	0.09	98.1	93.2
HB1122	Cpx	53.24	16.89	2.42	20.54	3.00	1.34	0.76	0.08	0.05	0.22	98.5	92.6
HB1125	Cpx	52.93	17.32	2.42	21.33	2.60	1.27	0.47	0.04	0.02	0.05	98.4	92.8
HB1126	Cpx	54.02	15.04	2.31	19.00	3.66	2.23	2.22	0.06	0.09	0.34	99.0	92.1

$Mg\# = 100 \times \text{mol } Mg^{2+}/(Mg^{2+} + Fe^{2+})$.

lithospheric mantle. Therefore, the depleted isotopic compositions reflect the effect of reaction between old peridotites and asthenosphere-derived melt (Fig. 6).

Refractory peridotite (high Fo) should be lower in Rb/Sr and higher in Sm/Nd than primitive mantle due to the more incompatibility of Rb than Sr and Nd than Sm during partial melting (Adam and Green, 2006) and thus be lower in $^{87}Sr/^{86}Sr$ and higher $^{143}Nd/^{144}Nd$ ratios than fertile peridotite (low Fo) and primitive mantle. This is completely opposite to the observation that olivine Fo in the Cenozoic basalt-borne peridotite xenoliths from the Central Zone positively correlate with Sr isotope ratios and negatively correlate with Nd isotope ratios (Fig. 8). Therefore, the correlations between Sr–Nd isotopic compositions and olivine Fo, first discussed in the Hannuoba peridotites (Zhang et al., 2009), likely reflect different-degree refertilization of originally refractory precursors through reaction with asthenosphere-derived melts (Tang et al., 2008; Zhang et al., 2009).

Compilation of Sr and Nd isotopic compositions of peridotites reveals that very few samples from ancient cratonic mantle keep the characteristics of ancient melt residues, although their major-element compositions reflect an origin as melt residues (Menzies, 1990; Pearson, 1999). For example, Nd isotopes in peridotite xenoliths (Fig. 6) from global cratons range from high $^{143}Nd/^{144}Nd$ ratios, indicative of long-term parent–daughter depletion, to low $^{143}Nd/^{144}Nd$ ratios, requiring ancient parent–daughter enrichment.

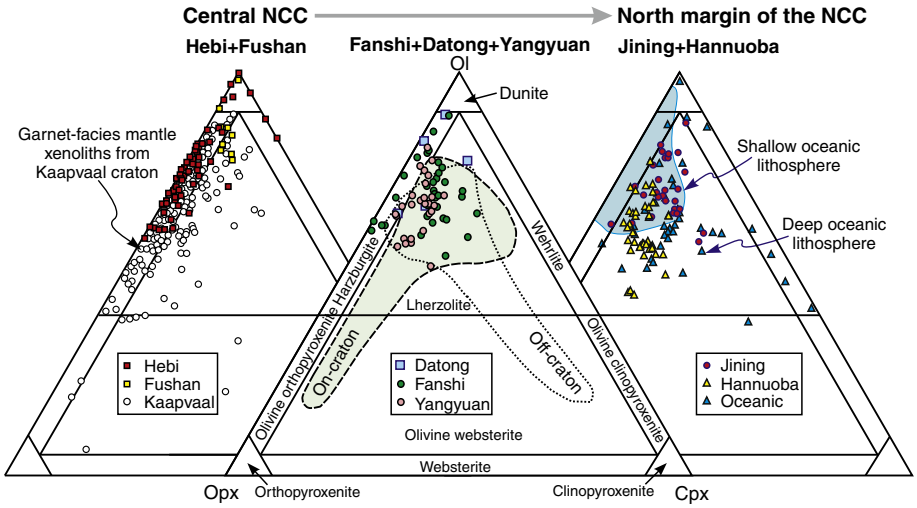

Fig. 2. Petrological classification of peridotites. On-craton and off-craton peridotite xenoliths, shallow (abyssal, ophiolitic peridotites) and deep oceanic lithosphere (basalt-borne xenoliths), and kimberlite-borne garnet-facies mantle xenoliths from the Kaapvaal craton, South Africa, are from Fan et al. (2000) and references therein. The 'deep' basalt-borne xenoliths from ocean basins (i.e. deep lithosphere) are similar to those from eastern China.
Data sources: Fushan (Xu et al., 2010), Hebi (Zheng et al., 2001, 2005; Liu et al., 2011; Tang et al., 2011 and this study), Fanshi (Tang et al., 2008; Xu et al., 2008b; Liu et al., 2011; Tang et al., 2011), Datong (Liu et al., 2011); Jining (Liu et al., 2011; Zhang et al., in press); Yangyuan (Xu et al., 2008b; Liu et al., 2011) and Hannuoba (Song and Frey, 1989; Fan et al., 2000; Rudnick et al., 2004; Tang et al., 2007; Liu et al., 2011).

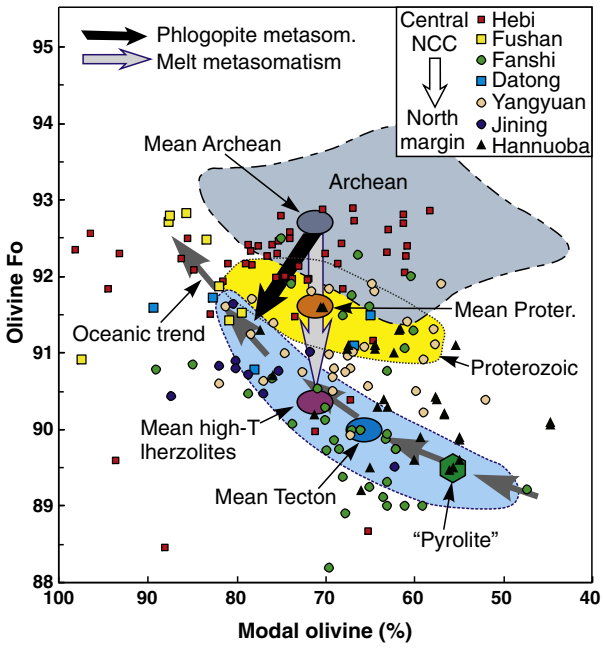

Fig. 3. Modal olivine vs. Fo contents plot showing the mean compositions of Archon, Proton and Tecton subcontinental lithospheric mantle, and high-T sheared lherzolite xenoliths from kimberlites. Two large arrows illustrate the effect of shallow phlogopite-related metasomatism, and the melt-related metasomatism responsible for the composition of the sheared xenoliths (Smith et al., 1991). The oceanic trend is the compositional trend from fertile lherzolite to depleted oceanic harzburgite (Boyd, 1989).The base chart is from Griffin et al. (2003). Data sources are as in Fig. 2.

Consequently, the greatly heterogeneous isotopic compositions in the lithospheric mantle beneath the Central Zone reflect the diversity in parent–daughter elemental fractionation in minerals coupled with ancient, multiple-stage histories of melt depletion and subsequent refertilization through melt influx. This is also supported by the elemental and isotopic characteristics of coexisting opx and cpx in the Hebi peridotites (Table 3, Fig. 6), which are similar to those in the

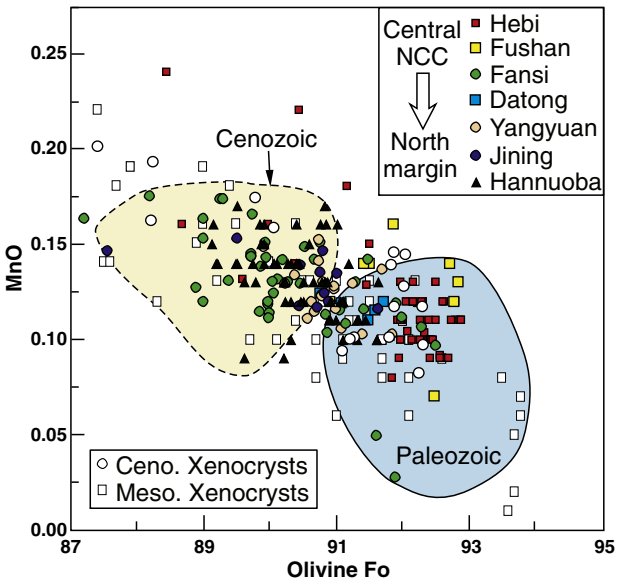

Fig. 4. Fo vs. MnO of olivine from the peridotites, compared with olivine xenocrysts in the Cenozoic Xiyang–Pingding basalts (Tang et al., 2004) and Mesozoic Shatuo gabbros (Ying et al., 2010) and peridotite xenoliths entrained in the Paleozoic kimberlites and Cenozoic basalts on the eastern NCC (Zheng et al., 1998, 2001). Data sources in addition to those designated in Fig. 2 include Hannuoba data from Fan and Hooper (1991) and Chen et al. (2001).

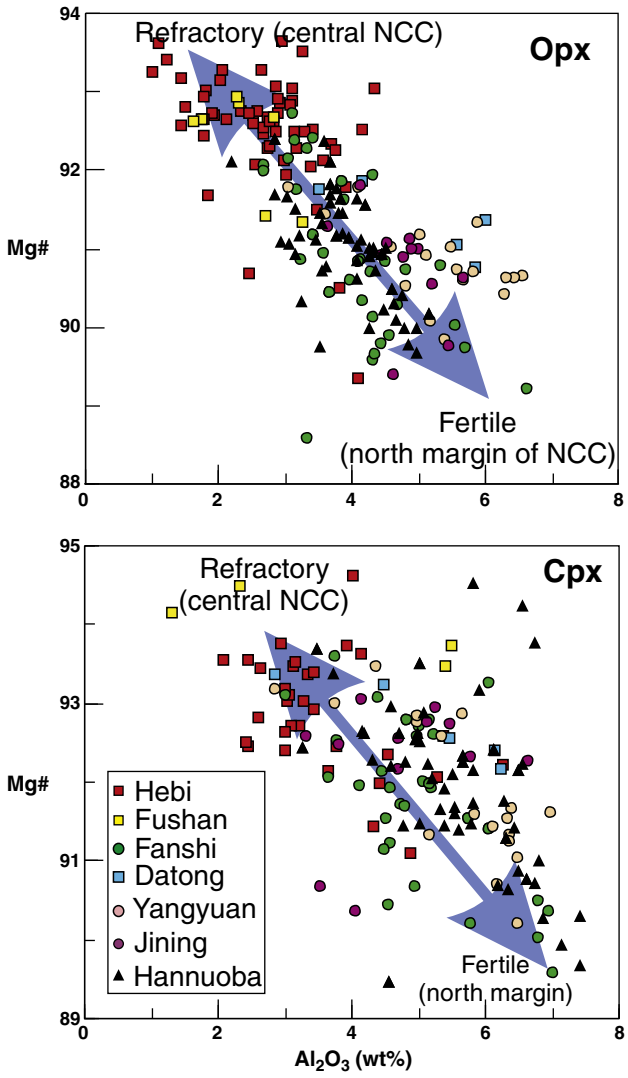

Fig. 5. Mg# vs. Al_2O_3 of opx and cpx in the mantle xenoliths from the Central Zone and the West Block of the NCC. Data sources are as in Fig. 3.

Fanshi peridotites, indicating multiple melt/fluid–peridotite interactions (Tang et al., 2011).

6.3. Re–Os isotopic data and nature of the lithospheric mantle

The Re–Os system has proven to be particularly useful in tracing the geochemical evolution of mantle rocks and in defining the chronology of mantle differentiation (Walker et al., 1989; Shirey and Walker, 1998). Nevertheless, an increasing number of studies have found that the Re–Os system in cratonic peridotites can be disturbed by peridotite–melt reaction, especially when reaction preceded eruption by large time intervals (Pearson et al., 1998; Alard et al., 2002; Zhang et al., 2008, 2009).

Sulfides from a mantle peridotite that underwent melt depletion and refertilization events may have a wide range of Re–Os model ages, reflecting different generations of "old" sulfides (residual after melt depletion) and later sulfide melts (interstitial sulfides related to melt/fluid metasomatism) (Pearson et al., 1999, 2002; Alard et al., 2002; Aulbach et al., 2004; Griffin et al., 2004; Xu et al., 2008a; Zhang et al., 2008, 2009; Harvey et al., 2010). This implies that the bulk-rock Re and Os budget will be controlled by the relative contributions from these sulfide populations, which are dependent on melt/rock ratios and the degree of S-saturation of the percolating melt during the refertilization of lithosphere (Reisberg et al., 2005;

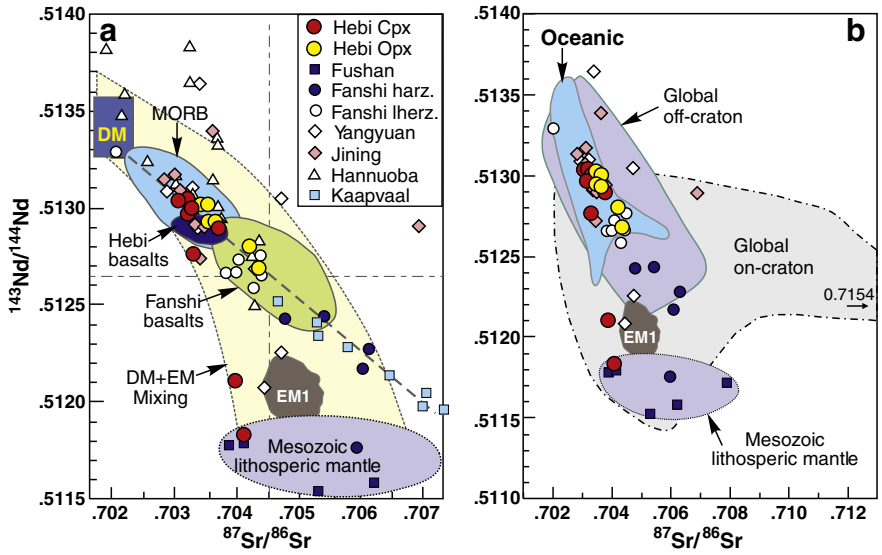

Fig. 6. (a) Sr and Nd isotope ratios in cpx and opx from the peridotites, together with the published data for peridotite xenoliths.
Data sources in addition to this study: cpx in peridotite xenoliths from Hannuoba (Song and Frey, 1989; Tatsumoto et al., 1992; Fan et al., 2000; Rudnick et al., 2004; Tang et al., 2011), Fanshi (Tang et al., 2008; Xu et al., 2008b; Tang et al., 2011), Yangyuan (Ma and Xu, 2006; Xu et al., 2008b), Jining peridotites (Zhang et al., in press) and the Kaapvaal craton, South Africa (Menzies and Murthy, 1980); Mesozoic lithospheric mantle beneath the Central Zone of the NCC (Zhang et al., 2004; Wang et al., 2006; Xu et al., 2010); Cenozoic Fanshi and Hebi host basalts (Tang et al., 2006, 2011, unpublished data); DM, MORB and EM1 (Zindler and Hart, 1986). The field roughly drawn denotes the DM-EM1 mixing trend.
(b) Oceanic peridotites and mantle peridotites from global on- and off-craton locations (Fan et al., 2000 and references therein).

Zhang et al., 2009; Xiao and Zhang, 2011). As a result, melt percolation could lead to significant changes in the Os isotopic compositions of the refertilized peridotites. Thus, whole-rock Os isotope compositions reflect the mixtures of different generations of sulfides. Therefore, the significant variability in Os isotopic compositions of sulfides within individual peridotite samples calls into question the significance of many published whole-rock "depletion ages" (Pearson et al., 2002).

Re–Os isotopic ages in the peridotite xenoliths from the NCC vary greatly, with Re-depletion model ages (T_{RD}) ranging from 0 to 3.0 Ga and Re–Os model ages (T_{MA}) of 0–3.5 Ga (Fig. 9). For example, most of the Hannuoba peridotites have Proterozoic whole-rock Re–Os model ages, resembling the Cenozoic basalt–host peridotites from other localities on the North China Craton (Fig. 9). However, the in situ T_{RD} and T_{MA} model ages of sulfides in the Hannuoba samples show a larger range, from Archean to Phanerozoic model ages, than the whole-rock ages of the peridotites, strongly indicating that the whole-rock ages are not the true formation ages of the peridotites, but the mixing ages of multiple generations of sulfides (Pearson et al., 2002; Griffin et al., 2004; Xu et al., 2008a; Zhang et al., 2009). The T_{RD} ages of these peridotites apparently correlate with olivine Fo (Fig. 9), which is traditionally explained as melting trend (Griffin et al., 2004). Alternatively, this correlation could also reflect the reaction trend of a depleted residue with asthenosphere-derived melts (Zhang et al., 2009). The refertilization of peridotites could lower the Fo of olivine (Zhang, 2005; Griffin et al., 2009) and result in the positive correlations between Re abundances and Al_2O_3 and Yb contents in the peridotites by additions of Fe, Al, Yb and Re (Zhang et al., 2009). Therefore, the correlation between T_{RD} ages and olivine Fo may reflect the combined results of partial melting and refertilization processes and the latter lowered the T_{RD} ages of the peridotites due to the additions of Re and less radiogenic Os or younger sulfide

Table 3
Sr and Nd isotopic compositions of cpx and opx in the peridotite xenoliths.

Sample	Rb (ppm)	Sr (ppm)	Sm (ppm)	Nd (ppm)	$^{87}Rb/^{86}Sr$	$^{87}Sr/^{86}Sr$	2σ	$^{147}Sm/^{144}Nd$	$^{143}Nd/^{144}Nd$	2σ
Cpx										
05HB68	0.003	144	0.355	4.72	0.0001	0.703092	10	0.0456	0.512942	9
05HB70	0.030	56.7	0.308	1.97	0.0015	0.703359	10	0.0944	0.513004	7
05HB72	0.660	315	4.01	20.9	0.0006	0.703246	10	0.1160	0.513039	6
HB1120	0.041	76.8	0.133	0.96	0.0015	0.704151	8	0.0841	0.511825	8
HB1121	0.000	167	0.247	2.25	0.0000	0.703862	8	0.0665	0.512144	12
HB1122	0.004	266	0.909	8.43	0.0000	0.703312	7	0.0652	0.512758	7
HB1125	0.003	161	0.506	5.88	0.0001	0.703242	8	0.0521	0.512960	10
HB1126	0.004	479	6.65	26.9	0.0000	0.703715	14	0.1494	0.512896	9
Opx										
05HB68	0.013	1.37			0.0276	0.703529	10			
05HB70	0.010	1.27	0.019	0.073	0.0234	0.703454	15	0.1604	0.513005	7
05HB72	0.017	2.85	0.063	0.207	0.0172	0.703560	10	0.1844	0.513003	24
HB1120	0.007	1.49			0.0144	0.704055	11			
HB1121	0.013	1.37			0.0277	0.703891	10			
HB1122	0.011	1.37	0.010	0.094	0.0230	0.704394	35	0.0664	0.512655	12
HB1125	0.015	9.91			0.0045	0.704829	10			
HB1126	0.035	4.25	0.073	0.231	0.0241	0.703576	13	0.1921	0.512920	8
05HB09	0.039	1.99	0.451	0.070	0.0561	0.704215	17	3.9155	0.512795	7
HB1128	0.081	8.77	0.070	0.325	0.0268	0.703655	11	0.1293	0.512907	7

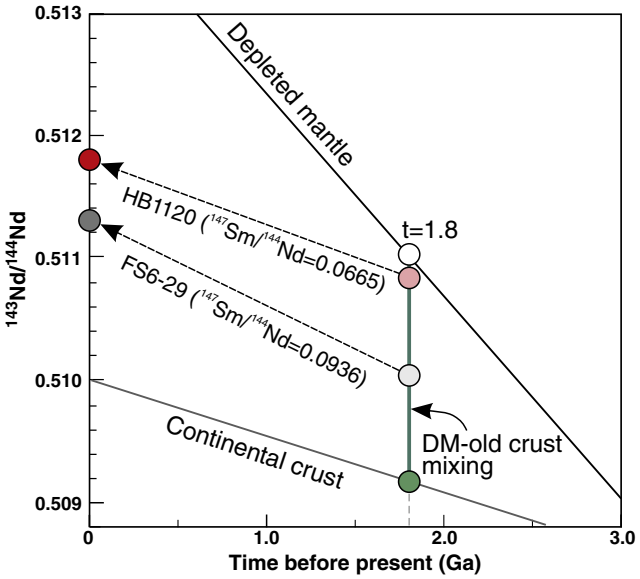

Fig. 7. The evolution of $^{143}Nd/^{144}Nd$ with time in the HB1120 (this study) and sample FS6–29 (Xu et al., 2010). DM-old crust mixing represents the assumed modification of the samples by recycled crustal materials at 1.8 Ga. The $^{143}Nd/^{144}Nd$ of the samples at 1.8 Ga were calculated based on the decay constant of ^{147}Sm (6.54×10^{-12}), $^{143}Nd/^{144}Nd$ of chondrite (0.512638) and the measured $^{143}Nd/^{144}Nd$ and Sm and Nd contents of the samples.

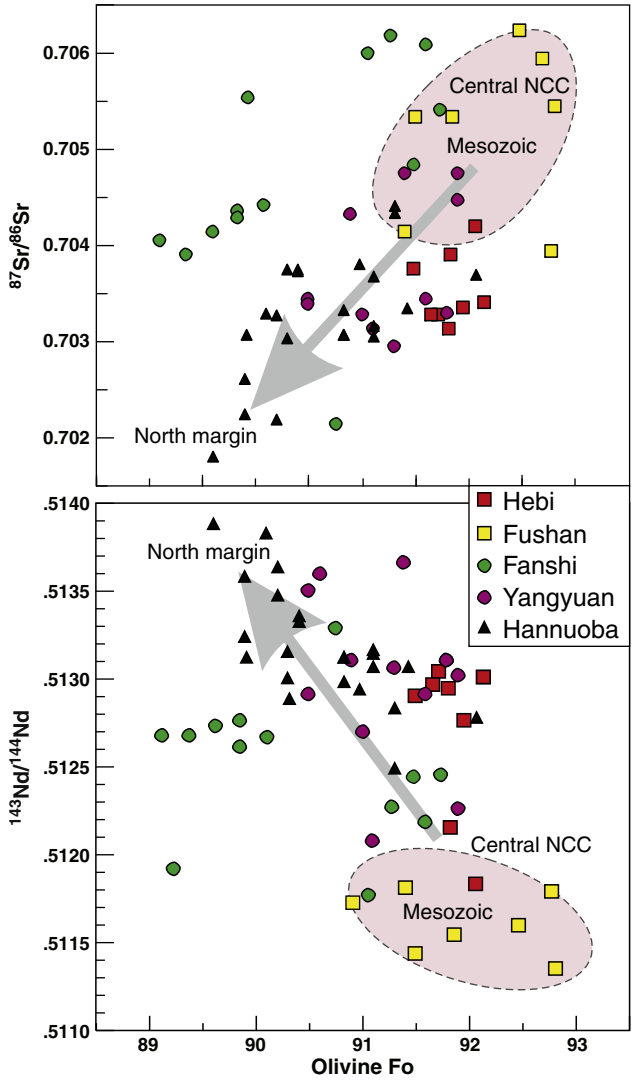

Fig. 8. Olivine Fo vs. Sr and Nd isotope ratios in cpx from the peridotites. Data sources are as in Fig. 6.

introduction, which could obliterate the evidence of old ages (Griffin et al., 2004).

The Re–Os isotopic data of Paleozoic kimberlite-borne xenoliths demonstrated that Archean lithospheric mantle existed beneath the eastern NCC during the Paleozoic (Gao et al., 2002; Wu et al., 2006; Zhang et al., 2008; Chu et al., 2009b). However, most of the peridotite xenoliths hosted by the Cenozoic basalts have Proterozoic T_{RD} and T_{MA} ages, with only a few xenoliths having Phanerozoic ages (Fig. 9). The scarcity of Archean T_{RD} ages may reflect that nearly all the Archean lithospheric mantle beneath the eastern NCC has been replaced (Gao et al., 2002; Wu et al., 2006; Chu et al., 2009b) or refertilized by multiple-stage influx of melts (Xu et al., 2008a; Zhang et al., 2008, 2009; Xiao and Zhang, 2011). In contrast, some peridotites in the Mesozoic and Cenozoic basaltic rocks in the Central Zone of the NCC have whole-rock (Xu et al., 2008b) or sulfide (Zheng et al., 2007; Xu et al., 2008a) T_{RD} ages of Archean, reflecting the existence of Archean mantle beneath this region. However, the wide range in T_{RD} ages observed in single peridotite and their sulfides may reflect progressive modification of the lithospheric mantle by fertile materials (Xu et al., 2008a), as is well documented for the peridotites from other regions of the world (Pearson et al., 1999, 2002; Alard et al., 2002; Griffin et al., 2004; Harvey et al., 2010). As a result, the T_{RD} ages for most of the samples from the North China Craton may reflect the mixing of different-generation sulfides generated by refertilization processes.

As a result, most of the peridotite xenoliths from the Central Zone, including Hebi, Fushan, Fanshi, Yangyuan, Datong, Jining and Hannuoba localities are relatively fertile in compositions (Figs. 3–5) and bear a resemblance to the "oceanic" lithosphere (Fan et al., 2000), but they are likely the fragments of refertilized Archean lithospheric mantle.

6.4. Constraints on the destruction of the NCC

The mineralogy, elemental and isotopic geochemistry of peridotite xenoliths entrained in the Mesozoic and Cenozoic igneous rocks from the NCC indicate that the present lithospheric mantle beneath the Central Zone is highly heterogeneous, which is likely produced from an Archean lithosphere by refertilization via multistage additions of melt. The early-stage melt may be derived from recycled crustal materials, and the later-stage melt be mainly derived from the asthenosphere. The refertilization processes could mask, even totally obliterate the Archean refractory signatures of parts of the lithosphere, and rejuvenate the Archean mantle by lowering the Re–Os model ages of refertilized peridotites (Zhang et al., 2008, 2009; Xiao and Zhang, 2011).

The peridotites from Fushan and Hebi in the central NCC are mainly refractory harzburgites with minor lherzolites (Fig. 2). Their extremely variable Sr–Nd isotopic ratios (Fig. 6) and Archean–Paleoproterozoic T_{RD} ages (Fig. 9) reflect low-degree modification of the Archean lithospheric mantle beneath the central NCC. In contrast, the peridotites from the Hannuoba and Jining in the northern margin of the craton are almost fertile lherzolites (Fig. 5) with depleted Sr–Nd isotopic compositions (Figs. 6 and 8) and Proterozoic–Phanerozoic T_{RD} ages (Fig. 9), indicating high-degree refertilization of the mantle lithosphere (Tang et al., 2008; Zhang et al., 2009, in press). One peridotite from Jining has radiogenic $^{87}Sr/^{86}Sr$ (up to 0.707, Fig. 6), likely implying the modification of oceanic crust (Zhang et al., in press). This is consistent with the observation of Santosh (2010) providing evidence for imbrication of oceanic plate lithostratigraphy from the Inner Mongolia suture zone (Fig. 1).

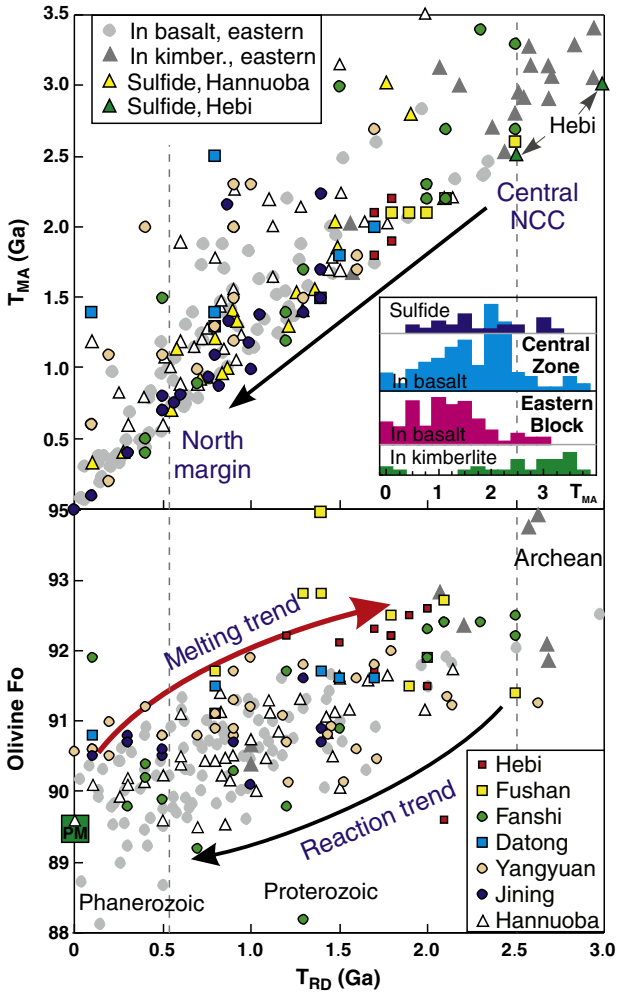

Fig. 9. Diagrams of T_{MA} and Fo of olivine vs. T_{RD} model ages of peridotite xenoliths and in situ analyses of sulfides from the NCC. Inset shows histogram of the T_{MA} ages. Data sources in addition to this study: Hannuoba peridotites (Gao et al., 2002; Xia et al., 2004; Zhang et al., 2009; Liu et al., 2011); Fushan, Datong and Hebi peridotites (Liu et al., 2011); Jining (Liu et al., 2011; Zhang et al., in press); Fanshi and Yangyuan peridotites (Xu et al., 2008b; Liu et al., 2011); In situ ages of sulfides in Hannuoba and Hebi peridotites (Zheng et al., 2007; Xu et al., 2008a); peridotite xenoliths entrained in the Cenozoic basalts (Gao et al., 2002; Wu et al., 2003, 2006; Chu et al., 2009b) and Paleozoic kimberlites from the NCC (Gao et al., 2002; Wu et al., 2006; Zhang et al., 2008; Chu et al., 2009b).

Compared to the Hannuoba peridotites, the Yangyuan and Fanshi xenoliths are mainly lherzolites with minor harzburgite, and have enriched Sr–Nd isotopic compositions and Archean–Phanerozoic T_{RD} ages, implying relatively low-degree modification of the lithospheric mantle. Therefore, the spatially petrologic and geochemical variations of xenoliths suggest that the refertilization of ancient lithospheric mantle by melt additions became stronger from the interior to the north margin of the NCC (Zhang, 2009) (Figs. 2–9).

For the whole North China Craton, it experienced a series of subduction/collision events, as evidenced by the Paleozoic to Triassic Qinling–Dabie ultrahigh-pressure belt in south (Li et al., 1993), the Tianshan–Inner Mongolia–Daxing'anling orogen in north (Xiao et al., 2003; Zhang et al., 2003) and the Mesozoic–Cenozoic subduction of Pacific plate in east. These events could intensively modify the subcontinental lithospheric mantle by igneous refertilization via multistage peridotite–melt reactions (Zhang et al., 2002, 2003; Xu et al., 2008a; Zhang et al., 2009; Zhang et al., 2010a, 2010b; Tang et al., 2011, 2012), leading to the highly heterogeneity of the mantle.

7. Conclusions

Mineral element and Sr–Nd isotopic compositions of the peridotite xenoliths from the Cenozoic Hebi basalts in the Central Zone of the NCC, coupled with previously published petrologic and isotopic data of mantle xenoliths from the eastern NCC, allow us to draw the following conclusions:

(1) The Hebi harzburgite xenoliths are refractory in mineral compositions and highly variable in mineral Sr–Nd isotopic compositions, ranging from MORB-like to EM1-type mantle. They are the residues of Archean lithospheric mantle beneath this region.
(2) The present lithospheric mantle beneath the Central Zone of the NCC is highly heterogeneous in mineral and geochemical compositions, likely produced by refertilization via multiple additions of melts.
(3) The refertilization of the lithospheric mantle became stronger from the interior to the margin of the craton, which was closely related to multiple subduction/collision events of circum-craton plates.

Acknowledgments

We would like to express our gratitude to Qian Mao and Yu-Guang Ma for their assistance with EPMA analyses and Jing-Hui Guo with isotopic analyses at the State Key Laboratory of Lithospheric Evolution, Institute of Geology and Geophysics, Chinese Academy of Sciences. We gratefully acknowledge the constructive reviews of S. Aulbach and an anonymous reviewer and editorial handling by Editors, which helped us to improve the presentation. This work was financially supported by the National Science Foundation of China (Grants 91014007, 41073028 and 40773026).

References

Adam, J., Green, T., 2006. Trace element partitioning between mica- and amphibole-bearing garnet lherzolite and hydrous basanitic melt: 1. Experimental results and the investigation of controls on partitioning behaviour. Contributions to Mineralogy and Petrology 152, 1–17.
Alard, O., Griffin, W.L., Pearson, N.J., Lorand, J.P., O'Reilly, S.Y., 2002. New insights into the Re–Os systematics of sub-continental lithospheric mantle from in situ analysis of sulphides. Earth and Planetary Science Letters 203, 651–663.
Aulbach, S., Griffin, W.L., O'Reilly, S.Y., McCandless, T.E., 2004. Genesis and evolution of the lithospheric mantle beneath the Buffalo Head Terrane, Alberta (Canada). Lithos 77, 413–451.
Beyer, E.E., Griffin, W.L., O'Reilly, S.Y., 2006. Transformation of Archaean lithospheric mantle by refertilization: evidence from exposed peridotites in the Western Gneiss Region, Norway. Journal of Petrology 47, 1611–1636.
Boyd, F.R., 1989. Compositional distinction between oceanic and cratonic lithosphere. Earth and Planetary Science Letters 96, 15–26.
Chen, S.H., O'Reilly, S.Y., Zhou, X.H., Griffin, W.L., Zhang, G.H., Sun, M., Feng, J.L., Zhang, M., 2001. Thermal and petrological structure of the lithosphere beneath Hannuoba, Sino–Korean Craton, China: evidence from xenoliths. Lithos 56, 267–301.
Chen, L., Zheng, T., Xu, W., 2006. A thinned lithospheric image of the Tanlu Fault Zone, eastern China: constructed from wave equation based receiver function migration. Journal of Geophysical Research 111, B09312. doi:10.1029/2005jb003974.
Chu, Z.Y., Chen, F.K., Yang, Y.H., Guo, J.H., 2009a. Precise determination of Sm, Nd concentrations and Nd isotopic compositions at the nanogram level in geological samples by thermal ionization mass spectrometry. Journal of Analytical Atomic Spectrometry 24, 1534–1544.
Chu, Z.Y., Wu, F.Y., Walker, R.J., Rudnick, R.L., Pitcher, L., Puchtel, I.S., Yang, Y.H., Wilde, S.A., 2009b. Temporal evolution of the lithospheric mantle beneath the eastern North China Craton. Journal of Petrology 50, 1857–1898.
Dobbs, P.N., Duncan, D.J., Hu, S., Shee, S.R., Colgan, E., Brown, M.A., Smith, C.B., Allsopp, H.L., 1994. The geology of the Mengyin kimberlites, Shandong, China. In: Meyer, H.O.A., Leonardos, O.H. (Eds.), Diamonds: Characterization, Genesis and Exploration, Proceedings of the 5th International Kimberlite Conference. CPRM, Brasilia, pp. 106–115.
Fan, Q.C., Hooper, P.R., 1991. The Cenozoic basaltic rocks of eastern China: petrology and chemical composition. Journal of Petrology 32, 765–810.
Fan, W.M., Menzies, M.A., 1992. Destruction of aged lower lithosphere and accretion of asthenosphere mantle beneath eastern China. Geotectonica et Metallogenia 16, 171–180.

Fan, W.M., Zhang, H.F., Baker, J., Jarvis, K.E., Mason, P.R.D., Menzies, M.A., 2000. On and off the north China craton: where is the Archaean keel? Journal of Petrology 41, 933–950.
Frey, F.A., Green, D.H., 1974. The mineralogy, geochemistry and origin of Iherzolite inclusions in Victorian basanites. Geochimica et Cosmochimica Acta 38, 1023–1059.
Gao, S., Rudnick, R.L., Carlson, R.W., McDonough, W.F., Liu, Y.S., 2002. Re–Os evidence for replacement of ancient mantle lithosphere beneath the North China craton. Earth and Planetary Science Letters 198, 307–322.
Gao, S., Rudnick, R.L., Yuan, H.L., Liu, X.M., Liu, Y.S., Xu, W.L., Ling, W.L., Ayers, J., Wang, X.C., Wang, Q.H., 2004. Recycling lower continental crust in the North China craton. Nature 432, 892–897.
Griffin, W.L., O'Reilly, S.Y., Ryan, C.G., 1992. Composition and thermal structure of the lithosphere beneath South Africa, Siberia and China: proton microprobe studies. International Symposium on Cenozoic Volcanic Rocks and Deep-seated Xenoliths of China and its Environs, Beijing, pp. 65–66.
Griffin, W.L., Zhang, A.D., O'Reilly, S.Y., Ryan, C.G., 1998. Phanerozoic evolution of the lithosphere beneath the Sino–Korean Craton. In: Flower, M.F.J., Chung, S.L., Lo, C.H., Lee, T.Y. (Eds.), Mantle Dynamics and Plate Interactions in East Asia. American Geophysical Union, Washington D.C., pp. 107–126.
Griffin, W.L., O'Reilly, S.Y., Abe, N., Aulbach, S., Davies, R.M., Pearson, N.J., Doyle, B.J., Kivi, K., 2003. The origin and evolution of Archean lithospheric mantle. Precambrian Research 127, 19–41.
Griffin, W.L., Graham, S., O'Reilly, S.Y., Pearson, N.J., 2004. Lithosphere evolution beneath the Kaapvaal Craton: Re–Os systematics of sulfides in mantle-derived peridotites. Chemical Geology 208, 89–118.
Griffin, W.L., O'Reilly, S.Y., Afonso, J.C., Begg, G.C., 2009. The composition and evolution of lithospheric mantle: a re-evaluation and its tectonic implications. Journal of Petrology 50, 1185–1204.
Harvey, J., Gannoun, A., Burton, K.W., Schiano, P., Rogers, N.W., Alard, O., 2010. Unravelling the effects of melt depletion and secondary infiltration on mantle Re–Os isotopes beneath the French Massif Central. Geochimica et Cosmochimica Acta 74, 293–320.
Kelemen, P.B., Hart, S.R., Bernstein, S., 1998. Silica enrichment in the continental upper mantle via melt/rock reaction. Earth and Planetary Science Letters 164, 387–406.
Kröner, A., Wilde, S.A., Li, J.H., Wang, K.Y., 2005. Ages and evolution of a Late Archean to Paleoproterozoic upper to lower crustal section in the Wutaishan/Hengshan/Fuping terrain of northern China. Journal of Asian Earth Sciences 24, 577–595.
Kusky, T.M., 2011. Geophysical and geological tests of tectonic models of the North China Craton. Gondwana Research 20, 26–35.
Li, S.G., Xiao, Y.L., Liou, D.L., Chen, Y.Z., Ge, N.J., Zhang, Z.Q., Sun, S.S., Cong, B.L., Zhang, R.Y., Hart, S.R., Wang, S.S., 1993. Collision of the North China and Yangtze Blocks and formation of coesite-bearing eclogite-timing and processes. Chemical Geology 109, 89–111.
Liu, J., Rudnick, R.L., Walker, R.J., Gao, S., Wu, F.Y., Piccoli, P.M., Yuan, H., Xu, W.L., Xu, Y.G., 2011. Mapping lithospheric boundaries using Os isotopes of mantle xenoliths: an example from the North China Craton. Geochimica et Cosmochimica Acta 75, 3881–3902.
Ma, X., 1989. Atlas of Active Faults in China. Seismologic Press, Beijing.
Ma, J.L., Xu, Y.G., 2006. Old EM1-type enriched mantle under the middle North China Craton as indicated by Sr and Nd isotopes of mantle xenoliths from Yangyuan, Hebei Province. Chinese Science Bulletin 51, 1343–1349.
Menzies, M.A., 1990. Effects of small volume melts. Nature 343, 312–313.
Menzies, M., Murthy, V.R., 1980. Enriched mantle: Nd and Sr isotopes in diopsides from kimberlite nodules. Nature 283, 634–636.
Menzies, M.A., Xu, Y.G., 1998. Geodynamics of the North China Craton. In: Flower, M.F.J., Chung, S.L., Lo, C.H., Lee, T.Y. (Eds.), Mantle Dynamics and Plate Interactions in East Asia. American Geophysical Union, Washington D.C., pp. 155–165.
Menzies, M.A., Fan, W.M., Zhang, M., 1993. Palaeozoic and Cenozoic lithoprobes and the loss of >120 km of Archaean lithosphere, Sino–Korean craton, China. In: Prichard, H.M., Alabaster, T., Harris, N.B.W., Neary, C.R. (Eds.), Magmatic Processes and Plate Tectonics. Geological Society of London, Special Publication, pp. 71–81.
Menzies, M., Xu, Y.G., Zhang, H.F., Fan, W.M., 2007. Integration of geology, geophysics and geochemistry: a key to understanding the North China Craton. Lithos 96, 1–21.
O'Reilly, S.Y., Griffin, W.L., Poudjom, Y.H., Morgan, P., 2001. Are lithosphere forever? Tracking changes in subcontinental lithospheric mantle through time. GSA Today 11, 4–10.
Pearson, D.G., 1999. Evolution of cratonic lithospheric mantle: an isotopic perspective. In: Fei, Y., Berka, C.M., Mysen, B.O. (Eds.), Mantle Petrology: Field Observations and High-Pressure Experimentation: A Tribute to Francis R (Joe) Boyd. The Geochemical Society Special Publication, pp. 57–78.
Pearson, D.G., Shirey, S.B., Harris, J.W., Carlson, R.W., 1998. Sulphide inclusions in diamonds from the Koffiefontein kimberlite, S Africa: constraints on diamond ages and mantle Re–Os systematics. Earth and Planetary Science Letters 160, 311–326.
Pearson, D.G., Shirey, S.B., Bulanova, G.P., Carlson, R.W., Milledge, H.J., 1999. Re–Os isotope measurements of single sulfide inclusions in a Siberian diamond and its nitrogen aggregation systematics. Geochimica et Cosmochimica Acta 63, 703–711.
Pearson, N.J., Alard, O., Griffin, W.L., Jackson, S.E., O'Reilly, S.Y., 2002. In situ measurement of Re–Os isotopes in mantle sulfides by laser ablation multicollector-inductively coupled plasma mass spectrometry: analytical methods and preliminary results. Geochimica et Cosmochimica Acta 66, 1037–1050.
Reisberg, L., Zhi, X.C., Lorand, J.P., Wagner, C., Peng, Z.C., Zimmermann, C., 2005. Re–Os and S systematics of spinel peridotite xenoliths from east central China: evidence for contrasting effects of melt percolation. Earth and Planetary Science Letters 239, 286–308.
Rudnick, R.L., Gao, S., Ling, W.L., Liu, Y.S., McDonough, W.F., 2004. Petrology and geochemistry of spinel peridotite xenoliths from Hannuoba and Qixia, North China Craton. Lithos 77, 609–637.
Santosh, M., 2010. Assembling North China Craton within the Columbia supercontinent: the role of double-sided subduction. Precambrian Research 178, 149–167.
Santosh, M., Tsunogae, T., Li, J.H., Liu, S.J., 2007a. Discovery of sapphirine-bearing Mg–Al granulites in the North China Craton: implications for Paleoproterozoic ultrahigh temperature metamorphism. Gondwana Research 11, 263–285.
Santosh, M., Wilde, S.A., Li, J.H., 2007b. Timing of Paleoproterozoic ultrahigh-temperature metamorphism in the North China Craton: evidence from SHRIMP U–Pb zircon geochronology. Precambrian Research 159, 178–196.
Santosh, M., Sajeev, K., Li, J.H., Liu, S.J., Itaya, T., 2009. Counterclockwise exhumation of a hot orogen: the Paleoproterozoic ultrahigh-temperature granulites in the North China Craton. Lithos 110, 140–152.
Santosh, M., Zhao, D., Kusky, T., 2010. Mantle dynamics of the Paleoproterozoic North China Craton: a perspective based on seismic tomography. Journal of Geodynamics 49, 39–53.
Santosh, M., Liu, S.J., Tsunogae, T., Li, J.H., 2011. Paleoproterozoic ultrahigh-temperature granulites in the North China Craton: implications for tectonic models on extreme crustal metamorphism. Precambrian Research. doi:10.1016/j.precamres.2011.1005.1003.
Shirey, S.B., Walker, R.J., 1998. The Re–Os isotopic system in cosmochemistry and igneous geochemistry. Annual Reviews of Earth and Planetary Sciences 26, 425–500.
Smith, D., Griffin, W.L., Ryan, C.G., Sie, S.H., 1991. Trace-element zonation in garnets from the thumb — heating and melt infiltration below the Colorado Plateau. Contributions to Mineralogy and Petrology 107, 60–79.
Song, Y., Frey, F.A., 1989. Geochemistry of peridotite xenoliths in basalt from Hannuoba, eastern China: implications for subcontinental mantle heterogeneity. Geochimica et Cosmochimica Acta 53, 97–113.
Tang, Y.J., Zhang, H.F., Ying, J.F., 2004. High-Mg olivine xenocrysts entrained in Cenozoic basalts in central Taihang Mountains: relicts of old lithospheric mantle. Acta Petrologica Sinica 20, 1243–1252.
Tang, Y.J., Zhang, H.F., Ying, J.F., 2006. Asthenosphere–lithospheric mantle interaction in an extensional regime: implication from the geochemistry of Cenozoic basalts from Taihang Mountains, North China Craton. Chemical Geology 233, 309–327.
Tang, Y.J., Zhang, H.F., Nakamura, E., Moriguti, T., Kobayashi, K., Ying, J.F., 2007. Lithium isotopic systematics of peridotite xenoliths from Hannuoba, North China Craton: implications for melt–rock interaction in the considerably thinned lithospheric mantle. Geochimica et Cosmochimica Acta 71, 4327–4341.
Tang, Y.J., Zhang, H.F., Ying, J.F., Zhang, J., Liu, X.M., 2008. Refertilization of ancient lithospheric mantle beneath the central North China Craton: evidence from petrology and geochemistry of peridotite xenoliths. Lithos 101, 435–452.
Tang, Y.J., Zhang, H.F., Nakamura, E., Ying, J.F., 2011. Multistage melt/fluid–peridotite interactions in the refertilized lithospheric mantle beneath the North China Craton: constraints from the Li–Sr–Nd isotopic disequilibrium between minerals of peridotite xenoliths. Contributions to Mineralogy and Petrology 161, 845–861.
Tang, Y.J., Zhang, H.F., Deloule, E., Su, B.X., Ying, J.F., Xiao, Y., Hu, Y., 2012. Slab-derived lithium isotopic signatures in mantle xenoliths from northeastern North China Craton. Lithos. doi:10.1016/j.lithos.2011.12.001.
Tatsumoto, M., Basu, A.R., Huang, W.K., Wang, J.W., Xie, G.H., 1992. Sr, Nd, and Pb isotopes of ultramafic xenoliths in volcanic-rocks of eastern China: enriched components EMI and EMII in subcontinental lithosphere. Earth and Planetary Science Letters 113, 107–128.
Walker, R.J., Carlson, R.W., Shirey, S.B., Boyd, F.R., 1989. Os, Sr, Nd, and Pb isotope systematics of southern African peridotite xenoliths: implications for the chemical evolution of subcontinental mantle. Geochimica et Cosmochimica Acta 53, 1583–1595.
Wang, Y.J., Fan, W.M., Zhang, H.F., Peng, T.P., 2006. Early Cretaceous gabbroic rocks from the Taihang Mountains: implications for a paleosubduction-related lithospheric mantle beneath the central North China Craton. Lithos 86, 281–302.
Wilshire, H.G., Shervais, J.W., 1975. Al-augite and Cr-diopside ultramafic xenoliths in basaltic rocks from western United States. Physics and Chemistry of the Earth 9, 257–272.
Wu, F.Y., Walker, R.J., Ren, X.W., Sun, D.Y., Zhou, X.H., 2003. Osmium isotopic constraints on the age of lithospheric mantle beneath northeastern China. Chemical Geology 196, 107–129.
Wu, F.Y., Walker, R.J., Yang, Y.H., Yuan, H.L., Yang, J.H., 2006. The chemical–temporal evolution of lithospheric mantle underlying the North China Craton. Geochimica et Cosmochimica Acta 70, 5013–5034.
Xia, Q.X., Zhi, X.C., Meng, Q., Zheng, L., Peng, Z.C., 2004. The trace element and Re–Os isotopic geochemistry of mantle-derived peridotite xenoliths from Hannuoba: nature and age of SCLM beneath the area. Acta Petrologica Sinica 20, 1215–1224 (in Chinese with English abstract).
Xiao, Y., Zhang, H.F., 2011. Effects of melt percolation on platinum group elements and Re–Os systematics of peridotites from the Tan–Lu fault zone, eastern North China Craton. Journal of the Geological Society of London 168, 1201–1214.
Xiao, W.J., Windley, B., Hao, J., Zhai, M.G., 2003. Accretion leading to collision and the Permian Solonker suture, Inner Mongolia, China: termination of the Central Asian orogenic belt. Tectonics 22. doi:10.1029/2202 TC001484.
Xu, Y.G., 2001. Thermo-tectonic destruction of the Archean lithospheric keel beneath the Sino–Korean Craton in China: evidence, timing and mechanism. Physics and Chemistry of the Earth (A) 26, 747–757.
Xu, Y.G., 2002. Evidence for crustal components in the mantle and constraints on crustal recycling mechanisms: pyroxenite xenoliths from Hannuoba, North China. Chemical Geology 182, 301–322.
Xu, X.S., O'Reilly, S.Y., Griffin, W.L., Zhou, X.M., Huang, X.L., 1998. The nature of the Cenozoic lithosphere of Nushan, eastern China. In: Flower, M.F.J., Chung, S.L., Lo, C.H., Lee, T.Y. (Eds.), Mantle Dynamics and Plate Interactions in East Asia. American Geophysical Union, Washington D.C., pp. 167–196.

Xu, Y.G., Chung, S.L., Ma, J.L., Shi, L.B., 2004. Contrasting Cenozoic lithospheric evolution and architecture in the western and eastern Sino–Korean craton: constrains from geochemistry of basalts and mantle xenoliths. Journal of Geology 112, 593–605.
Xu, X.S., Griffin, W.L., O'Reilly, S.Y., Pearson, N.J., Geng, H.Y., Zheng, J.P., 2008a. Re–Os isotopes of sulfides in mantle xenoliths from eastern China: progressive modification of lithospheric mantle. Lithos 102, 43–64.
Xu, Y.G., Blusztajn, J., Ma, J.L., Suzuki, K., Liu, J.F., Hart, S.R., 2008b. Late Archean to early Proterozoic lithospheric mantle beneath the western North China craton: Sr–Nd–Os isotopes of peridotite xenoliths from Yangyuan and Fansi. Lithos 102, 25–42.
Xu, W., Yang, D., Gao, S., Pei, F., Yu, Y., 2010. Geochemistry of peridotite xenoliths in Early Cretaceous high-Mg# diorites from the Central Orogenic Block of the North China Craton: the nature of Mesozoic lithospheric mantle and constraints on lithospheric thinning. Chemical Geology 270, 257–273.
Yang, J.H., Wu, F.Y., Wilde, S.A., 2003. A review of the geodynamic setting of large-scale Late Mesozoic gold mineralization in the North China craton: an association with lithospheric thinning. Ore Geology Reviews 23, 125–152.
Ying, J.F., Zhang, H.F., Tang, Y.J., 2010. Zoned olivine xenocrysts in a late Mesozoic gabbro from the southern Taihang Mountains: implications for old lithospheric mantle beneath the central North China Craton. Geological Magazine 147, 161–170.
Yuan, X.C., 1996. Atlas of Geophysics in China. Geological Publishing House, Beijing.
Zhai, M.G., Santosh, M., 2011. The early Precambrian odyssey of the North China Craton: a synoptic overview. Gondwana Research 20, 6–25.
Zhang, H.F., 2005. Transformation of lithospheric mantle through peridotite–melt reaction: a case of Sino–Korean craton. Earth and Planetary Science Letters 237, 768–780.
Zhang, H.F., 2009. Peridotite–melt interaction: a key point for the destruction of cratonic lithospheric mantle. Chinese Science Bulletin 54, 3417–3437.
Zhang, H.F., Sun, M., Zhou, X.H., Fan, W.M., Zhai, M.G., Ying, J.F., 2002. Mesozoic lithosphere destruction beneath the North China Craton: evidence from major-, trace-element and Sr–Nd–Pb isotope studies of Fangcheng basalts. Contributions to Mineralogy and Petrology 144, 241–253.
Zhang, H.F., Sun, M., Zhou, X.H., Zhou, M.F., Fan, W.M., Zheng, J.P., 2003. Secular evolution of the lithosphere beneath the eastern North China Craton: evidence from Mesozoic basalts and high-Mg andesites. Geochimica et Cosmochimica Acta 67, 4373–4387.
Zhang, H.F., Sun, M., Zhou, M.F., Fan, W.M., Zhou, X.H., Zhai, M.G., 2004. Highly heterogeneous late Mesozoic lithospheric mantle beneath the north China Craton: evidence from Sr–Nd–Pb isotopic systematics of mafic igneous rocks. Geological Magazine 141, 55–62.
Zhang, J., Zhao, G.C., Sun, M., Wilde, S.A., Li, S.Z., Liu, S.W., 2006. High-pressure mafic granulites in the Trans-North China Orogen: tectonic significance and age. Gondwana Research 9, 349–362.
Zhang, H.F., Nakamura, E., Kobayashi, K., Zhang, J., Ying, J.F., Tang, Y.J., Niu, L.F., 2007. Transformation of subcontinental lithospheric mantle through peridotite–melt reaction: evidence from a highly fertile mantle xenolith from the North China craton. International Geology Review 49, 658–679.
Zhang, H.F., Goldstein, S., Zhou, X.H., Sun, M., Zheng, J.P., Cai, Y., 2008. Evolution of subcontinental lithospheric mantle beneath eastern China: Re–Os isotopic evidence from mantle xenoliths in Paleozoic kimberlites and Mesozoic basalts. Contributions to Mineralogy and Petrology 155, 271–293.
Zhang, H.F., Goldstein, S.L., Zhou, X.H., Sun, M., Cai, Y., 2009. Comprehensive refertilization of lithospheric mantle beneath the North China Craton: further Os–Sr–Nd isotopic constraints. Journal of the Geological Society of London 166, 249–259.
Zhang, H.F., Deloule, E., Tang, Y.J., Ying, J.F., 2010a. Melt/rock interaction in remains of refertilized Archean lithospheric mantle in Jiaodong Peninsula, North China Craton: Li isotopic evidence. Contributions to Mineralogy and Petrology 160, 261–277.
Zhang, H.F., Nakamura, E., Kobayashi, K., Ying, J.F., Tang, Y.J., 2010b. Recycled crustal melt injection into lithospheric mantle: implication from cumulative composite and pyroxenite xenoliths. International Journal of Earth Sciences 99, 1167–1186.
Zhang, H.F., Ying, J.F., Tang, Y.J., Li, X.H., Feng, C., Santosh, M., 2011. Phanerozoic reactivation of the Archean North China Craton through episodic magmatism: evidence from zircon U–Pb geochronology and Hf isotopes from the Liaodong Peninsula. Gondwana Research 19, 446–459.
Zhang, H.F., Sun, Y.L., Tang, Y.J., Xiao, Y., Zhang, W.H., Zhao, X.M., Santosh, M., Menzies, M.A., in press. Melt-peridotite interaction in the Pre-cambrian mantle beneath the western North China Craton: Petrology, geochemistry and Sr, Nd and Re isotopes. Lithos. doi:10.1016/j.lithos.2012.01.027.
Zhao, G.C., Cawood, P.A., Wilde, S.A., Sun, M., 2000. Metamorphism of basement rocks in the Central Zone of the North China craton: implications for Paleoproterozoic tectonic evolution. Precambrian Research 103, 55–88.
Zhao, G.C., Wilde, S.A., Sun, M., Li, S.Z., Li, X.P., Zhang, J., 2008. SHRIMP U–Pb zircon ages of granitoid rocks in the Lüliang Complex: implications for the accretion and evolution of the Trans-North China Orogen. Precambrian Research 160, 213–226.
Zhao, G.C., Wilde, S.A., Guo, J.H., Cawood, P.A., Sun, M., Li, X.P., 2010a. Single zircon grains record two Paleoproterozoic collisional events in the North China Craton. Precambrian Research 177, 266–276.
Zhao, G.C., Wilde, S.A., Zhang, J., 2010b. New evidence from seismic imaging for subduction during assembly of the North China craton: comment. Geology 38, e206.
Zhao, X.M., Zhang, H.F., Zhu, X.K., Tang, S.H., Tang, Y.J., 2010c. Iron isotope variations in spinel peridotite xenoliths from North China Craton: implications for mantle metasomatism. Contributions to Mineralogy and Petrology 160, 1–14.
Zheng, J.P., O'Reilly, S.Y., Griffin, W.L., Lu, F.X., Zhang, M., 1998. Nature and evolution of Cenozoic lithospheric mantle beneath Shandong peninsula, Sino–Korean craton, eastern China. International Geology Review 40, 471–499.
Zheng, J.P., O'Reilly, S.Y., Griffin, W.L., Lu, F.X., Zhang, M., Pearson, N.J., 2001. Relict refractory mantle beneath the eastern North China block: significance for lithosphere evolution. Lithos 57, 43–66.
Zheng, J.P., Griffin, W.L., O'Reilly, S.Y., Liou, J.G., Zhang, R.Y., Lu, F.X., 2005. Late Mesozoic–Eocene mantle replacement beneath the eastern North China craton: evidence from the Paleozoic and Cenozoic peridotite xenoliths. International Geology Review 47, 457–472.
Zheng, J.P., Griffin, W.L., O'Reilly, S.Y., Yang, J.S., Li, T.F., Zhang, M., Zhang, R.Y., Liou, J.G., 2006. Mineral chemistry of peridotites from Paleozoic, Mesozoic and Cenozoic lithosphere: constraints on mantle evolution beneath eastern China. Journal of Petrology 47, 2233–2256.
Zheng, J.P., Griffin, W.L., O'Reilly, S.Y., Yu, C.M., Zhang, H.F., Pearson, N., Zhang, M., 2007. Mechanism and timing of lithospheric modification and replacement beneath the eastern North China Craton: peridotitic xenoliths from the 100 Ma Fuxin basalts and a regional synthesis. Geochimica et Cosmochimica Acta 71, 5203–5225.
Zhou, X.H., Armstrong, R.L., 1982. Cenozoic volcanic rocks of eastern China — secular and geographic trends in chemistry and strontium isotopic composition. Earth and Planetary Science Letters 58, 301–329.
Zindler, A., Hart, S.R., 1986. Chemical geodynamics. Annual Reviews of Earth and Planetary Sciences 14, 493–571.